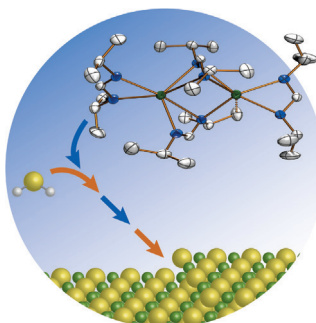


... of conjugated polymers is their solution processability with low cost. Conjugated polymers typically have flexible alkyl side chains for solubility in organic solvents, and J. Liu, L. Wang, and co-workers report in their Communication on page 10376 ff. soluble conjugated polymers bearing novel side chains, branched oligo(ethylene glycol). These polymers can be used in solution-processed polymer solar cells with high efficiency and near-IR response.

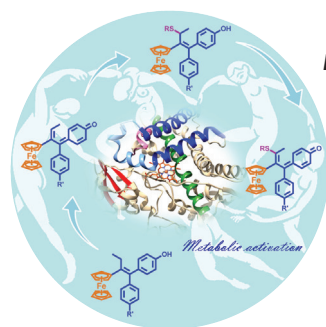
Atomic Layer Deposition

The use of volatile dimeric calcium(II) amidinate complexes as highly effective ALD precursors for the synthesis of uniform CaS thin films is reported by R. G. Gordon et al. in their Communication on page 10228 ff.



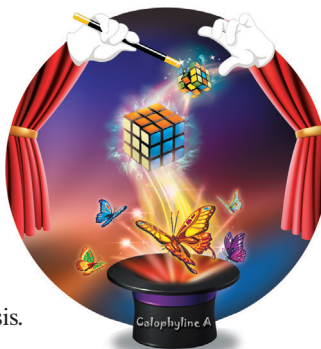
Bioinorganic Chemistry

In their Communication on page 10431 ff., G. Jaouen and co-workers describe the synthesis and behavior of organometallic antiproliferative compounds resulting from the addition of thiols to ferrocenyl quinone methides.



Skeletal Rearrangements

The first total synthesis of calophylline A is reported by L. Zu and co-workers in their Communication on page 10483 ff. An aza-pinacol rearrangement served as the key strategy in the synthesis.



How to contact us:

Editorial Office:

E-mail: angewandte@wiley-vch.de

Fax: (+49) 62 01-606-331

Telephone: (+49) 62 01-606-315

Reprints, E-Prints, Posters, Calendars:

Carmen Leitner

E-mail: chem-reprints@wiley-vch.de

Fax: (+49) 62 01-606-331

Telephone: (+49) 62 01-606-327

Copyright Permission:

Bettina Loycke

E-mail: rights-and-licences@wiley-vch.de

Fax: (+49) 62 01-606-332

Telephone: (+49) 62 01-606-280

Online Open:

Margitta Schmitt

E-mail: angewandte@wiley-vch.de

Fax: (+49) 62 01-606-331

Telephone: (+49) 62 01-606-315

Subscriptions:

www.wileycustomerhelp.com

Fax: (+49) 62 01-606-184

Telephone: 0800 1800536 (Germany only)
+44(0) 1865476721 (all other countries)

Advertising:

Marion Schulz

E-mail: mschulz@wiley-vch.de

Fax: (+49) 62 01-606-550

Telephone: (+49) 62 01-606-565

Courier Services:

Boschstrasse 12, 69469 Weinheim

Regular Mail:

Postfach 101161, 69451 Weinheim

Angewandte Chemie International Edition is a journal of the Gesellschaft Deutscher Chemiker (GDCh), the largest chemistry-related scientific society in continental Europe. Information on the various activities and services of the GDCh, for example, cheaper subscription to *Angewandte Chemie International Edition*, as well as applications for membership can be found at www.gdch.de or can be requested from GDCh, Postfach 900440, D-60444 Frankfurt am Main, Germany.

GDCh

GESELLSCHAFT
DEUTSCHER CHEMIKER

Get the **Angewandte App**
International Edition



Enjoy Easy Browsing and a New Reading Experience on Your Smartphone or Tablet

- Keep up to date with the latest articles in Early View.
- Download new weekly issues automatically when they are published.
- Read new or favorite articles anytime, anywhere.



Service

Spotlight on Angewandte's Sister Journals

10176–10179

Author Profile



"My favorite food is dumplings.

My favorite motto is "Where there's a will, there is a way". ..."

This and more about Xiaoyuan (Shawn) Chen can be found on page 10180.

Xiaoyuan (Shawn) Chen — 10180

News

Royal Society of Chemistry Prizes and Awards 2016 — 10181–10182



I. J. S. Fairlamb



T. Wirth



V. M. Rotello



J. A. Murphy



A. Weller



R. E. P. Winpenny



M. S. Hill



J. Zhu



A. J. Wilson

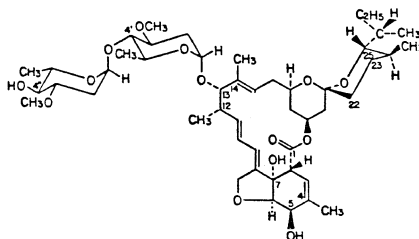


H. Wennemers

Nobel Lectures

Avermectins

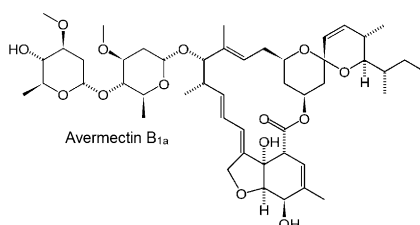
W. C. Campbell* — 10184–10189

Ivermectin: A Reflection on Simplicity
(Nobel Lecture)

Parasitic diseases including river blindness and lymphatic filariasis affect hundreds of millions of people annually. The discovery of the drug ivermectin has provided humankind with a powerful new means to combat these severe diseases. To a very large extent the drug was brought about by “simple” science.

Avermectins

S. Ōmura* — 10190–10209

A Splendid Gift from the Earth: The
Origins and Impact of the Avermectins
(Nobel Lecture)

Japanese soil was the origin of one of the most important drugs of the world: ivermectin. No other drug has such importance for the health of millions of people, particularly in the poor regions of the world. The discovery of the parent compounds of the avermectins is described first hand by S. Ōmura.

Malaria

Y. Tu* — 10210–10226

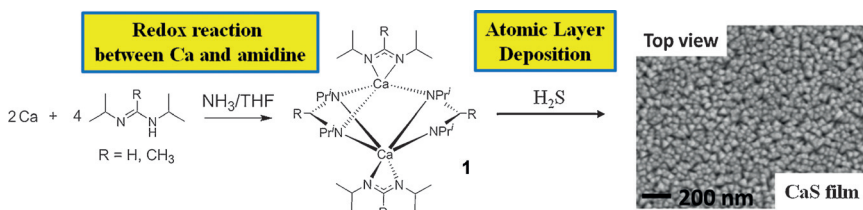
Artemisinin—A Gift from Traditional
Chinese Medicine to the World (Nobel
Lecture)

Malaria has long been a devastating and life-threatening global epidemic disease in human history. Artemisinin, the active substance against malaria, was first isolated and tested in the 1970s in China. The important role played by traditional Chinese medicine in the discovery of artemisinin is described by Y. Tu in her Nobel Lecture.



Communications

ALD Precursors

S. B. Kim, C. Yang, T. Powers, L. M. Davis,
X. Lou, R. G. Gordon* — 10228–10233Synthesis of Calcium(II) Amidinate
Precursors for Atomic Layer Deposition
through a Redox Reaction between
Calcium and Amidines

Fling the window open: Dimeric amidinate complexes **1** were obtained as volatile white crystals from a redox reaction between Ca metal and amidine ligands (see scheme). The vapor of the formamidinate complex was used for the synthesis

of conformal and uniform polycrystalline CaS films by ALD. With this complex, the ALD window was considerably wider and lower in temperature (150–280°C) than that observed with the most commonly used ALD precursor.

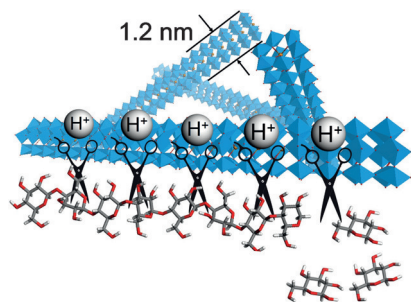
Frontispiece

For the USA and Canada:

ANGEWANDTE CHEMIE International Edition (ISSN 1433-7851) is published weekly by Wiley-VCH, PO Box 101161, 69451 Weinheim, Germany. US mailing agent: SPP, PO Box 437, Emigsville, PA 17318. Periodicals postage

paid at Emigsville, PA. US POSTMASTER: send address changes to *Angewandte Chemie*, John Wiley & Sons Inc., C/O The Sheridan Press, PO Box 465, Hanover, PA 17331. Annual subscription price for institutions: US\$ 16.862/14.051 (valid for print and electronic / print or

electronic delivery); for individuals who are personal members of a national chemical society prices are available on request. Postage and handling charges included. All prices are subject to local VAT/sales tax.



A molecular wire based on tungsten oxide with a diameter of 1.2 nm was synthesized. Acid sites were created in aqueous solution by calcination without collapse of the molecular wire structure. This material was applied for the hydrolysis of cellulosic biomass to produce hexose.

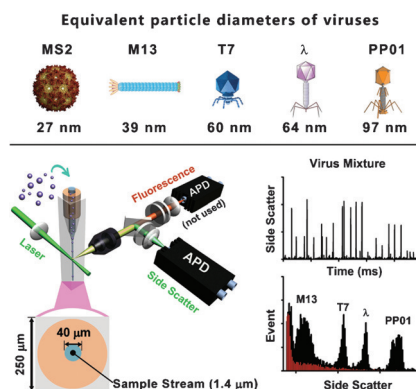
Molecular Wires

Z. Zhang,* M. Sadakane, N. Hiyoshi, A. Yoshida, M. Hara, W. Ueda* — 10234 – 10238

Acidic Ultrafine Tungsten Oxide Molecular Wires for Cellulosic Biomass Conversion



Virus detection: A laboratory-built high-sensitivity flow cytometer enables the precise quantification of the elastically scattered light intensity of individual viral particles with diameters down to 27 nm. This label-free approach provides a statistically reliable size distribution profile in 2–3 min, and a mixture of the bacteriophages M13, T7, λ , and PP01 could be baseline-resolved.



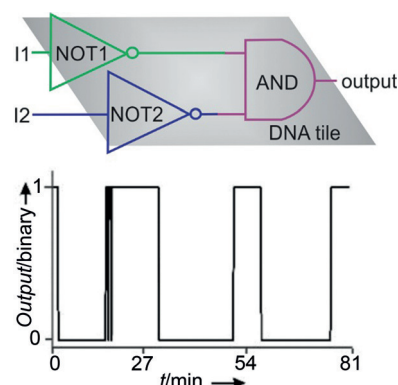
Light-Scattering Detection

L. Ma, S. Zhu, Y. Tian, W. Zhang, S. Wang, C. Chen, L. Wu, X. Yan* — 10239 – 10243

Label-Free Analysis of Single Viruses with a Resolution Comparable to That of Electron Microscopy and the Throughput of Flow Cytometry



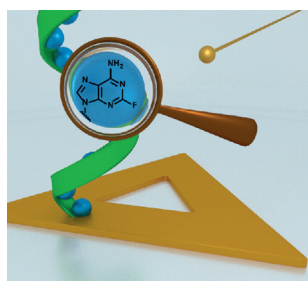
AND and NOR on DNA: Arrays of communicating DNA logic gates integrated in a single DNA tile were produced. The gates can process nucleic acid inputs in a reusable format.



Nucleic Acid Computation

Y. V. Gerasimova, D. M. Kolpashchikov* — 10244 – 10247

Towards a DNA Nanoprocessor: Reusable Tile-Integrated DNA Circuits



Breaking DNA: Strand breakage in DNA modified with 2-fluoroadenine induced by low-energy electrons is quantified using a DNA origami-based technique. The strand-break enhancement factor was in a similar range for all investigated electron energies.

DNA Radiosensitization

J. Rackwitz, J. Kopyra, I. Dąbkowska, K. Ebel, M. Ranković, A. R. Milosavljević, I. Bald* — 10248 – 10252

Sensitizing DNA Towards Low-Energy Electrons with 2-Fluoroadenine

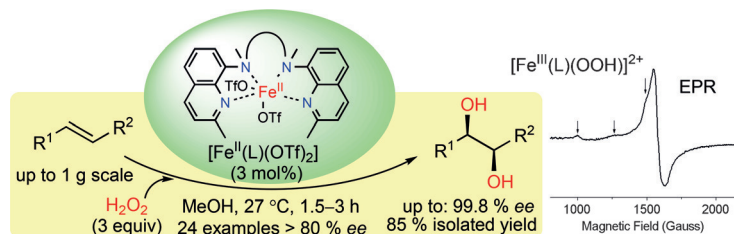


Alkene Hydroxylation

C. Zang, Y. Liu, Z.-J. Xu, C.-W. Tse,
X. Guan, J. Wei, J.-S. Huang,
C.-M. Che* 10253 – 10257



Highly Enantioselective Iron-Catalyzed *cis*-Dihydroxylation of Alkenes with Hydrogen Peroxide Oxidant via an Fe^{III}-OOH Reactive Intermediate



Earth-abundant ingredients:

[Fe^{II}(L)(OTf)₂]-catalyzed asymmetric *cis*-dihydroxylation of alkenes in a limiting amount with H₂O₂ as a terminal oxidant produces *cis*-diols in up to 99.8% *ee* with

85% yield. This “[Fe^{II}(L)(OTf)₂] + H₂O₂” method is applicable to both electron-deficient and -rich alkenes. Mechanistic studies suggest involvement of a chiral [Fe^{III}(L)(OOH)]²⁺ active species.

Organosilicon Chemistry

D. Pinchuk, J. Mathew, A. Kaushansky,
D. Bravo-Zhivotovskii,*
Y. Apeloig* 10258 – 10262



Isolation and Characterization, Including by X-ray Crystallography, of Contact and Solvent-Separated Ion Pairs of Silenyl Lithium Species

As changeable as a chameleon:

A reversible interconversion of a solvent separated and contact ion pair occurs by solvent exchange for R¹RC=SiR₂Li.

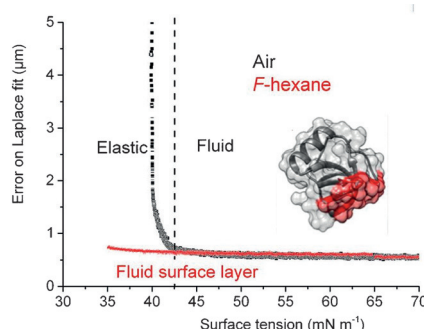
Characterization data, including the X-ray crystallographic structures, are detailed for these chromatically changeable species.

Interfacial Films

L. Gazzera, R. Milani, L. Pirrie,
M. Schmutz, C. Blanck, G. Resnati,
P. Metrangola,*
M. P. Krafft* 10263 – 10267



Design of Highly Stable Echogenic Microbubbles through Controlled Assembly of Their Hydrophobin Shell



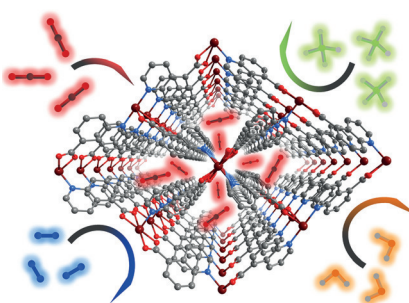
No-trouble microbubbles: A fluorocarbon gas prevents the fluid-to-solid state transition in HFBII hydrophobin 2D films. This new phenomenon allows the preparation of size-controlled, stable, and echogenic HFBII microbubbles with the potential for ultrasound imaging.

Metal–Organic Materials

K.-J. Chen, D. G. Madden, T. Pham,
K. A. Forrest, A. Kumar, Q.-Y. Yang, W. Xue,
B. Space, J. J. Perry IV, J.-P. Zhang,*
X.-M. Chen,
M. J. Zaworotko* 10268 – 10272

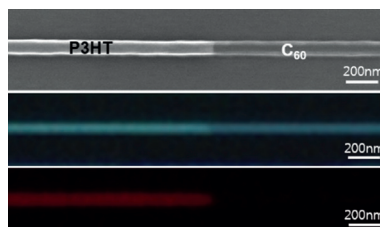


Tuning Pore Size in Square-Lattice Coordination Networks for Size-Selective Sieving of CO₂



Sieves you right: Crystal engineering of supramolecular isomers of [Cu(quinoline-5-carboxylate)₂]_n metal–organic materials enables the right pore-chemistry for ultra-high CO₂/N₂ and CO₂/CH₄ selectivity even in the presence of water vapor.

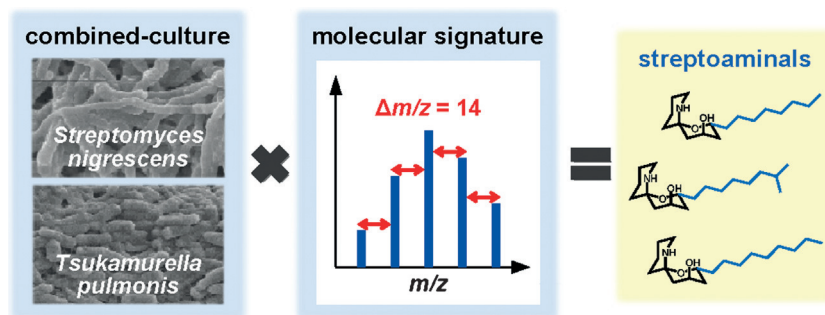
Junction box: Single-crystal organic axial P3HT/C₆₀ p–n heterojunction nanowires each having a well-defined junction region were fabricated by means of inkjet-assisted nanotransfer printing and were exploited for direct observation, by means of scanning photocurrent microscopy, of charge separation and depletion width in the junction region under external electric fields.



Molecular Electronics

K. S. Park, K. S. Lee, J. Baek, L. Lee, B. H. Son, Y. Koo Lee, Y. H. Ahn, W. I. Park, Y. Kang, M. M. Sung* 10273 – 10277

Observation of Charge Separation and Space-Charge Region in Single-Crystal P3HT/C₆₀ Heterojunction Nanowires



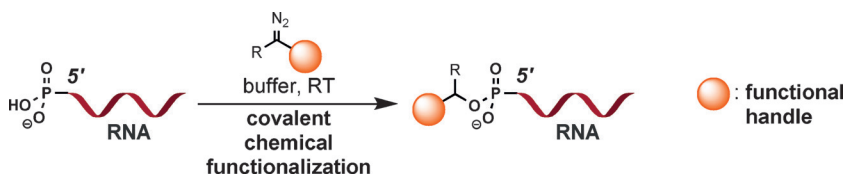
More than the sum of the parts: New antimicrobials were discovered using two approaches: the combined-culture

method, and molecular signature analysis by mass spectrometry.

Natural Products

R. Sugiyama, S. Nishimura,* T. Ozaki, S. Asamizu, H. Onaka, H. Kakeya* 10278 – 10282

Discovery and Total Synthesis of Streptoaminals: Antimicrobial [5,5]-Spirohemiaminals from the Combined-Culture of *Streptomyces nigrescens* and *Tsukamurella pulmonis*



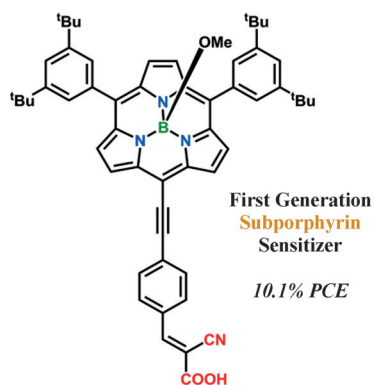
Conditions for selective alkylation of the 5'-phosphate of native RNA in aqueous media are reported. This method was applied to functionalize an oligonucleotide with both biotin and a small molecule

that endowed the RNA with binding affinity to the eukaryotic initiation factor 4E (eIF4E), thus confirming the ability to modulate RNA properties and suggesting applications in mRNA therapy.

Nucleotide Labelling

C. M. Gampe,* M. Hollis-Symynkywicz, F. Zécari 10283 – 10286

Covalent Chemical 5'-Functionalization of RNA with Diazo Reagents



Sensitivity training: The first generation of subphyrinatoboron(III)-based molecular sensitizers were tested in dye-sensitized solar cells (DSSCs). The most advanced prototype achieved a photon-to-current conversion efficiency value of 10.1%. Such an astonishing figure suggests the potential for subphyrinatoboron compounds in the field of DSSCs.

Sensitizers

G. Copley, D. Hwang, D. Kim,* A. Osuka* 10287 – 10291

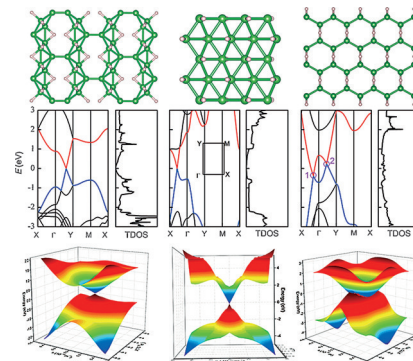
First-Generation Subphyrinatoboron(III) Sensitizers Surpass the 10% Power Conversion Efficiency Threshold



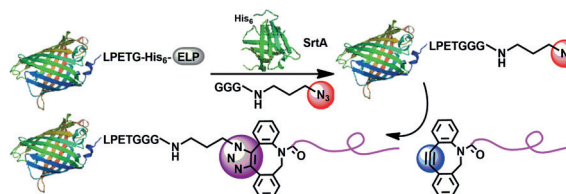
Boron Hydride Sheets

Y. Jiao, F. Ma, J. Bell, A. Bilic,
A. Du* 10292–10295Two-Dimensional Boron Hydride Sheets:
High Stability, Massless Dirac Fermions,
and Excellent Mechanical Properties

In an attempt to stabilize 2D boron layers, DFT and a global minimum search with the particle-swarm optimization method were used to predict four stable 2D boron hydride layers, namely *C2/m*, *Pbcm*, *Cmmm*, and *Pmmn* sheets. All of these structures are dynamically stable and possess a Dirac cone feature with massless Dirac fermions. The Fermi velocities for the *Pbcm* and *Cmmm* structures are even higher than that of graphene.



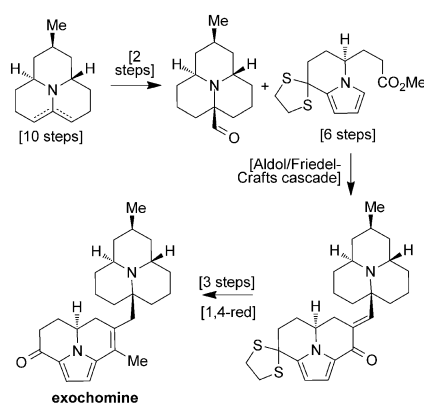
Protein Modification

Y. Pang, J. Liu, Y. Qi, X. Li,
A. Chilkoti* 10296–10300A Modular Method for the High-Yield
Synthesis of Site-Specific Protein–Polymer
Therapeutics

The site-specific and stoichiometric synthesis of protein/peptide–polymer therapeutics in high yield is enabled by a modular method that is based on a combination of recombinant expression, enzyme-

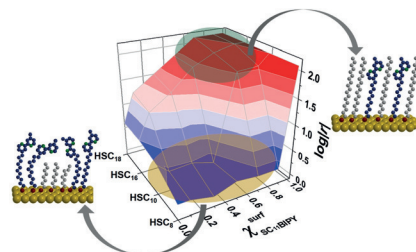
mediated ligation, and click chemistry. This approach is suitable for the conjugation of structurally diverse polymers to various protein and peptide drugs.

Natural Product Synthesis

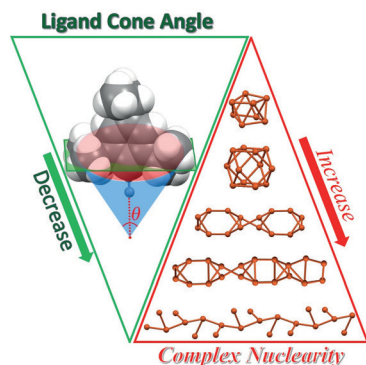
A. X. Gao, T. Hamada,
S. A. Snyder* 10301–10306The Enantioselective Total Synthesis of
Exochomine

Challenging chirality: Use of a distinct synthetic strategy to address the challenges in merging two different halves bearing a chiral center at their merger point has enabled access to the alkaloid exochomine in 16 steps. Key operations include the functionalization of a hindered iminium precursor, a unique aldol-based coupling cascade, and a robust protocol for 1,4-reduction in a hindered context where numerous side-reactions can occur.

Molecular Electronics

G. D. Kong, M. Kim, S. J. Cho,
H. J. Yoon* 10307–10311Gradients of Rectification: Tuning
Molecular Electronic Devices by the
Controlled Use of Different-Sized Diluents
in Heterogeneous Self-Assembled
Monolayers

Rectifying defects: A detailed study of the electrical behavior of binary surface-assembled monolayers (SAMs) composed of an organic rectifier, SC₁₁BIPY, and non-rectifying *n*-alkanethiolate diluents shows that the gradient behavior of rectification can be finely tuned by controlling the structure (specifically, the molecular length) of the diluent.

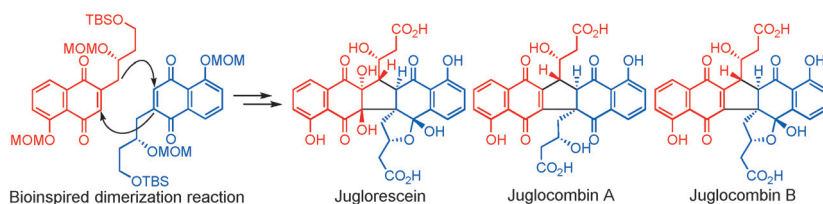


Knowing all the angles: By varying the steric bulk of alkynyl ligands, a Cu^I alkynyl polymer (Cu_∞) and clusters with various nuclearities (Cu_{4n}, *n* = 2–5) were formed and structurally characterized. Based on the crystal structures, a method to measure the cone angle of alkynyl ligands for evaluating their steric properties was proposed. The nuclearity of the complex was found to increase with decreasing alkynyl ligand cone angle.

Alkynyl Complexes

X.-Y. Chang, K.-H. Low, J.-Y. Wang,
J.-S. Huang, C.-M. Che* **10312–10316**

From Cluster to Polymer: Ligand Cone Angle Controlled Syntheses and Structures of Copper(I) Alkynyl Complexes



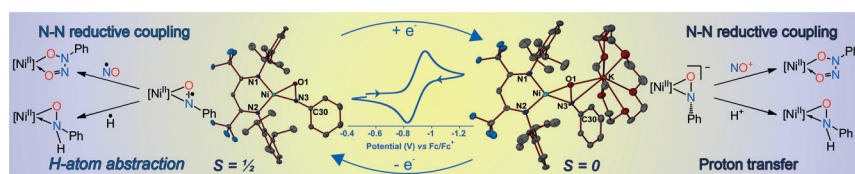
A jugl-ing act: Total syntheses of the natural naphthoquinone dimers juglorescein and juglocombins A and B were achieved through a biospired dimerization reaction. From known starting materials, juglorescein was synthesized in nine

steps and in 11% overall yield, and the common derivative of juglocombins A and B was synthesized in 14 steps and 3% overall yield. The relative and absolute configurations of the compounds were determined.

Fused-Ring Systems

S. Kamo, K. Yoshioka, K. Kuramochi,*
K. Tsubaki **10317–10320**

Total Syntheses of Juglorescein and Juglocombins A and B



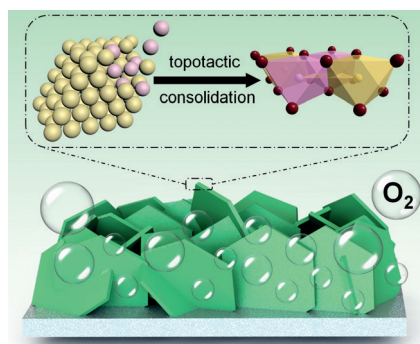
Isolation and characterization of two interconvertible reduced forms of the nitrosobenzene (PhNO) ligand bound to a common nickel(II) site reveals detailed

structure–reactivity relationships reminiscent of reduced forms of dioxygen (O₂) at mononuclear sites, including H-atom abstraction reactivity.

Nitroxyl Model Complexes

S. Kundu,* S. C. E. Stieber,* M. G. Ferrier,
S. A. Kozimor, J. A. Bertke,
T. H. Warren* **10321–10325**

Redox Non-Innocence of Nitrosobenzene at Nickel



Tactical topology: A topotactic consolidation of cobalt and zinc constituents into monocrystalline CoZn hydroxide nano-sheets is demonstrated for direct electrochemical oxygen evolution reactions.

Electrode Materials

J. Wang, C. F. Tan, T. Zhu,
G. W. Ho* **10326–10330**

Topotactic Consolidation of Monocrystalline CoZn Hydroxides for Advanced Oxygen Evolution Electrodes



Membrane Proteins

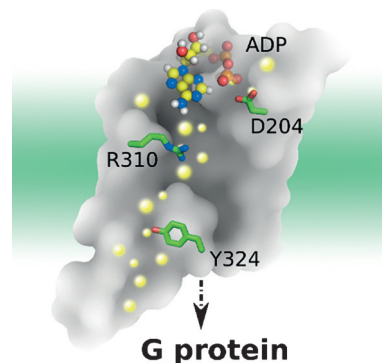


S. Yuan,* H. C. S. Chan, H. Vogel,
S. Filipek, R. C. Stevens,*
K. Palczewski* ————— 10331 – 10335



The Molecular Mechanism of P2Y₁
Receptor Activation

When the agonist ADP binds to the G-protein-coupled receptor P2Y₁R, it induces breakage of the ionic lock and increases the surface-accessible surface area, leading to a bulk water influx into the binding pocket. Consequently, the rotamer of highly conserved Y324⁷⁵³ undergoes a molecular switch and a continuous water channel forms inside the receptor resulting in P2Y₁R activation.

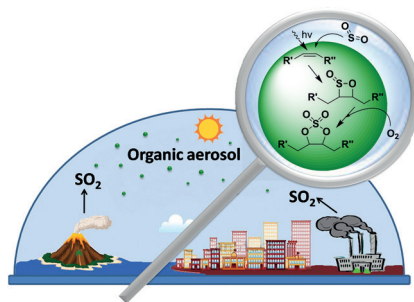


Atmospheric Chemistry

M. Passananti, L. Kong, J. Shang,
Y. Dupart, S. Perrier, J. Chen,
D. J. Donaldson,
C. George* ————— 10336 – 10339



Organosulfate Formation through the
Heterogeneous Reaction of Sulfur Dioxide
with Unsaturated Fatty Acids and Long-
Chain Alkenes



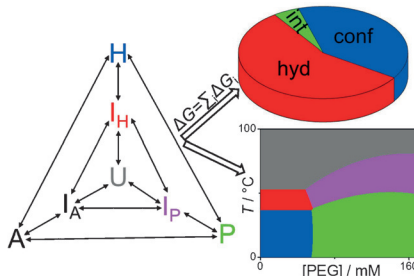
Atmospheric: Sulfur dioxide reacts with a range of fatty acids and long-chain alkenes to lead to organosulfur products. This reaction, which even takes place in the presence of ozone, is enhanced by light. The reaction products have the same composition as organosulfur compounds that have been detected in atmospheric aerosols.

G-Quadruplexes

M. Bončina, G. Vesnaver, J. B. Chaires,*
J. Lah* ————— 10340 – 10344



Unraveling the Thermodynamics of the
Folding and Interconversion of Human
Telomere G-Quadruplexes



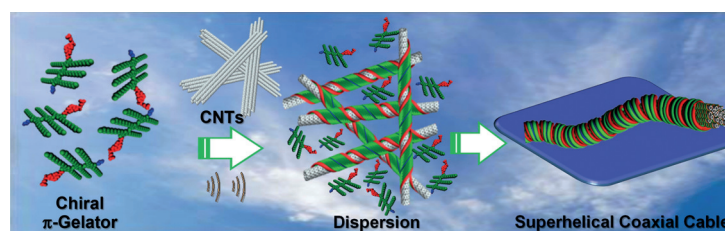
Thermodynamic analysis has enabled the construction of phase diagrams for describing the complex conformational phase space of a human telomere repeat DNA fragment. The analysis clarifies the driving forces for quadruplex folding and interconversion over a wide range of temperatures, salt, and co-solute concentrations and demonstrates their effect on the DNA structural features.

Chiral Carbon Nanocables

B. Vedhanarayanan, V. S. Nair, V. C. Nair,
A. Ajayaghosh* ————— 10345 – 10349

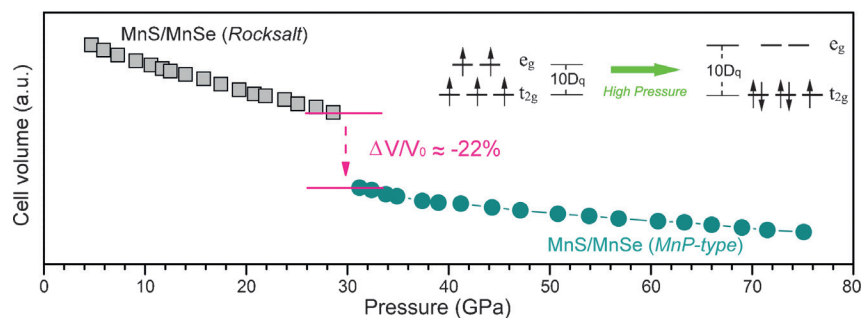


Formation of Coaxial Nanocables with
Amplified Supramolecular Chirality
through an Interaction between Carbon
Nanotubes and a Chiral π -Gelator



All wrapped up: The interaction of a chiral π -gelator with carbon nanotubes (CNTs) led to 20-fold amplification of the molecular chirality well below the critical aggregation concentration. Helical wrapping of

the gelator molecules around the nanotubes led to thick helical fibers composed of individually wrapped and coaxially aligned CNTs (see picture).



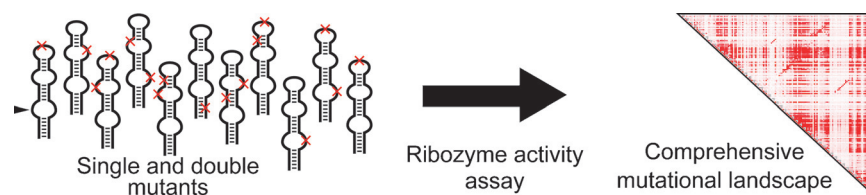
Under pressure: Giant lattice collapses during the pressure-driven phase transition in manganese chalcogenides are

associated with the formation of inter-metallic bonds and high-to-low spin state transition.

Manganese Chalcogenides

Y. Wang,* L. Bai, T. Wen, L. Yang, H. Gou, Y. Xiao, P. Chow, M. Pravica, W. Yang,* Y. Zhao* 10350–10353

Giant Pressure-Driven Lattice Collapse Coupled with Intermetallic Bonding and Spin-State Transition in Manganese Chalcogenides



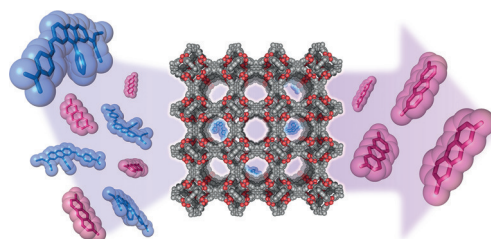
Ribozyme assay by sequencing: Deep sequencing was used to measure the activity of a self-cleaving ribozyme and all

of its single and double mutants (a total of 10296 mutants), revealing interesting features of the mutational landscape.

Ribozymes

S. Kobori, Y. Yokobayashi* 10354–10357

High-Throughput Mutational Analysis of a Twister Ribozyme



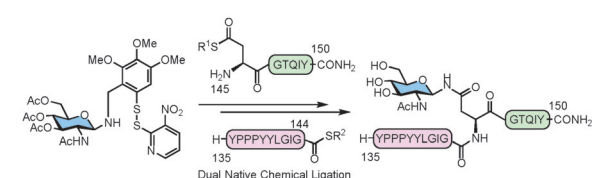
Stuck on U: Large cationic dyes and enzymes are adsorbed selectively over their anionic counterparts by a water-

stable anionic mesoporous metal-organic framework (MOF) based on uranium.

Uranium MOFs

P. Li, N. A. Vermeulen, X. Gong, C. D. Malliakas, J. F. Stoddart, J. T. Hupp, O. K. Farha* 10358–10362

Design and Synthesis of a Water-Stable Anionic Uranium-Based Metal-Organic Framework (MOF) with Ultra Large Pores



A practical approach towards *N*-glycopeptide synthesis using an auxiliary-mediated dual native chemical ligation (NCL) has been developed. The first NCL connects an *N*-linked glycosyl auxiliary to

the thioester side chain of an *N*-terminal aspartate oligopeptide. This intermediate undergoes a second NCL with a *C*-terminal thioester oligopeptide. Mild cleavage provides the desired *N*-glycopeptide.

N-Glycopeptide Synthesis

H. Chai, K. Le Mai Hoang, M. D. Vu, K. Pasunooti, C.-F. Liu, X.-W. Liu* 10363–10367

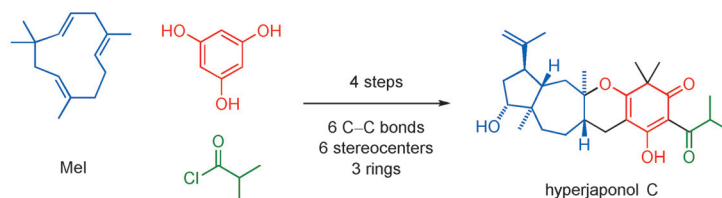
N-Linked Glycosyl Auxiliary-Mediated Native Chemical Ligation on Aspartic Acid: Application towards *N*-Glycopeptide Synthesis

**Biomimetic Synthesis**

H. C. Lam, J. T. J. Spence,
J. H. George* — 10368 – 10371



Biomimetic Total Synthesis of
Hyperjaponones A–E and Hyperjaponols A
and C



Chemical mimicry: A biomimetic oxidative hetero-Diels–Alder reaction was employed in the total syntheses of hyperjaponones A–E. Chemical mimicry of the proposed biosynthetic pathway for the

conversion of hyperjaponone A into hyperjaponol C allowed a concise total synthesis of hyperjaponol C to be completed in just four steps.

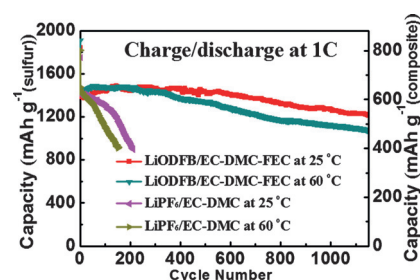
Lithium–Sulfur Batteries

Z. X. Xu, J. L. Wang, J. Yang,* X. W. Miao,
R. J. Chen, J. Qian,
R. R. Miao — 10372 – 10375



Enhanced Performance of a Lithium–
Sulfur Battery Using a Carbonate-Based
Electrolyte

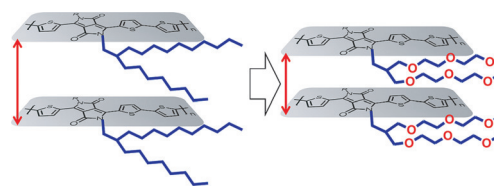
Energy storage: A lithium–sulfur battery system was designed using a carbonate-based electrolyte which not only overcomes the challenges of cyclability and life time at the lithium anode, but also matches the pyrolyzed polyacrylonitrile sulfur composite (S@pPAN) cathode perfectly. The battery system shows extraordinary electrochemical performances (see picture).

**Conjugated Polymers**

X. Chen, Z. Zhang, Z. Ding, J. Liu,*
L. Wang* — 10376 – 10380



Diketopyrrolopyrrole-based Conjugated
Polymers Bearing Branched
Oligo(Ethylene Glycol) Side Chains for
Photovoltaic Devices



Branched oligo(ethylene glycol) (OEG) was used as side chains of conjugated polymers. Compared to typical alkyl side chains, the branched OEG side chains led to smaller π – π distance of polymer back-

bone, redshifted absorption spectra, enhanced charge carrier mobilities, and higher dielectric constants. The resulting polymers exhibited outstanding photovoltaic performance in polymer solar cells.

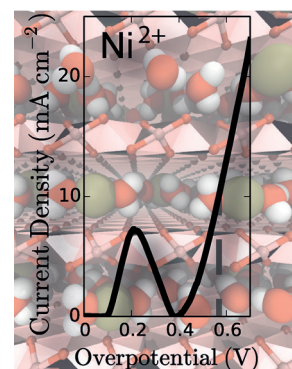
Front Cover**Oxygen Evolution Reaction**

A. C. Thenuwara, E. B. Cerkez,
S. L. Shumlas, N. H. Attanayake,
I. G. McKendry, L. Frazer, E. Borguet,
Q. Kang, R. C. Remsing, M. L. Klein,
M. J. Zdilla,
D. R. Strongin* — 10381 – 10385



Nickel Confined in the Interlayer Region of
Birnessite: an Active Electrocatalyst for
Water Oxidation

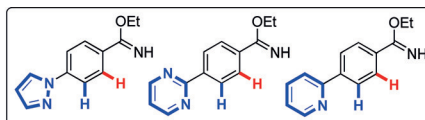
Confined interlayer waters: Tailoring the structure of interlayer water in birnessite by intercalating Ni^{2+} ions enhances electron transfer thus improving oxygen evolution reaction (OER) catalysis. These results could aid the synthesis of other OER catalysts that utilize layered or nanoporous materials.





- Fully tolerates strongly coordinating heterocycles
- Unique chemoselectivity

Strongly coordinating nitrogen heterocycles are fully tolerated by a versatile cobalt-catalyzed C–H amidation method, which provides access to structurally



- Inexpensive cobalt
- DG power analysis

complex quinazolines. The powers of various directing groups in cobalt-catalyzed C–H activation were thus delineated.

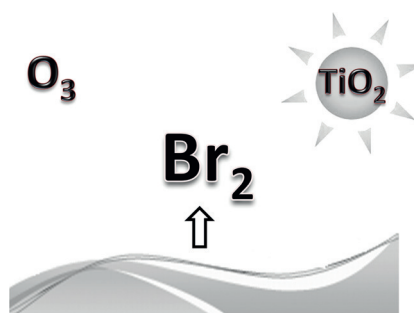
C–H Activation

H. Wang, M. M. Lorion,
L. Ackermann* 10386 – 10390

Overcoming the Limitations of C–H Activation with Strongly Coordinating N-Heterocycles by Cobalt Catalysis



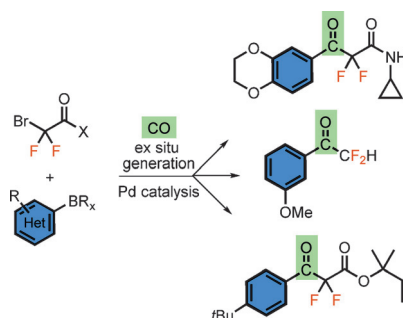
Brimming with bromine: Significant production of bromine was observed when acidic solutions of bromide were treated with a TiO₂ photocatalyst, and/or ozone. Bromine selectivities up to approximately 85 % were obtained with a corresponding atomic mass balance. The general process may be applied at a laboratory scale, or industrially as a cheap, safe, and environmentally sustainable alternative to current production methods.



Bromine Production

F. Parrino,* G. Camera Roda, V. Loddo,
L. Palmisano 10391 – 10395

Elemental Bromine Production by TiO₂ Photocatalysis and/or Ozonation

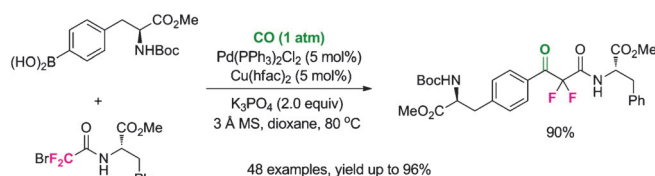


Yielding to pressure: The title reaction produces aryl α,α -difluoro- β -ketoamides and -esters from readily available difluorinated carboxylic acid derivatives by employing gaseous carbon monoxide. The method features low CO pressures and high functional-group tolerance. The fluorinated products can be transformed into a variety of fluoroalkylated structures.

Cross-Coupling

T. L. Andersen, M. W. Frederiksen,
K. Domino,
T. Skrydstrup* 10396 – 10400

Direct Access to α,α -Difluoroacylated Arenes by Palladium-Catalyzed Carbonylation of (Hetero)Aryl Boronic Acid Derivatives



Insertion of CO: A palladium-catalyzed carbonylation reaction of difluoroalkyl halides into ketones was developed (see picture). The resulting difluoroalkyl

ketones can serve as versatile building blocks for the synthesis of useful fluorinated compounds.

Carbonylation

H.-Y. Zhao, Z. Feng, Z. Luo,
X. Zhang* 10401 – 10405

Carbonylation of Difluoroalkyl Bromides Catalyzed by Palladium



**C–F Activation**

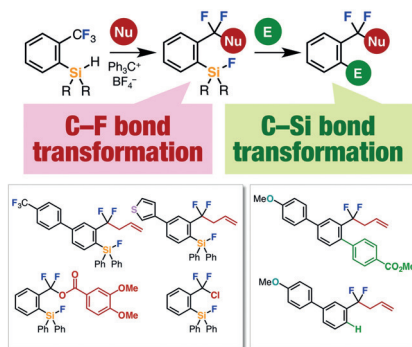
S. Yoshida,* K. Shimomori, Y. Kim,
T. Hosoya* 10406–10409



Single C–F Bond Cleavage of Trifluoromethylarenes with an *ortho*-Silyl Group



Inside Cover



One of the three: The transformation of a single C–F bond of trifluoromethylarenes bearing an *ortho*-hydrosilyl group is described. The activation of the hydrosilyl group with a trityl cation in the presence of nucleophiles enabled selective C–F bond functionalization, for example, by allylation, carboxylation, or chlorination. Further derivatization of the resulting fluorosilylarenes afforded various difluoromethylated arenes.

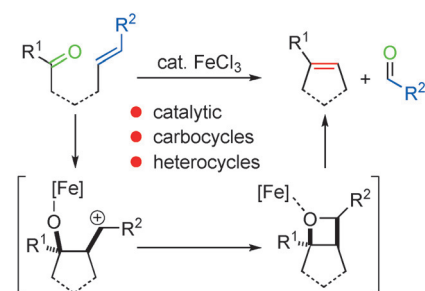
Metathesis

L. Ma, W. Li, H. Xi, X. Bai, E. Ma, X. Yan,
Z. Li* 10410–10413



FeCl₃-Catalyzed Ring-Closing Carbonyl–Olefin Metathesis

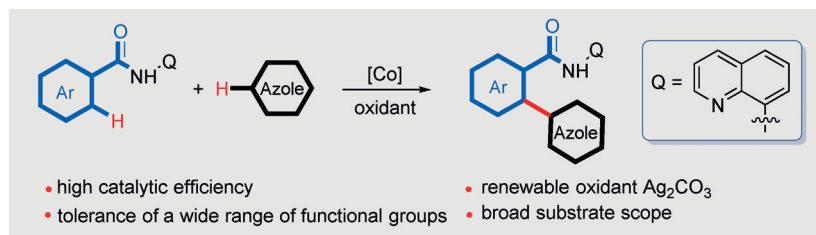
Ironing it out: The title reaction allows access to a range of carbo-/heterocyclic alkenes. The reaction is proposed to take place by FeCl₃-catalyzed oxetane formation followed by retro-ring-opening to deliver the metathesis products.

**C–C Cross-Coupling**

G. Tan, S. He, X. Huang, X. Liao, Y. Cheng,
J. You* 10414–10418



Cobalt-Catalyzed Oxidative C–H/C–H Cross-Coupling between Two Heteroarenes



A bidentate 8-quinolinyl ligand assists the cobalt-catalyzed title reaction between two (hetero)arenes exhibiting a broad substrate scope and a high tolerance level

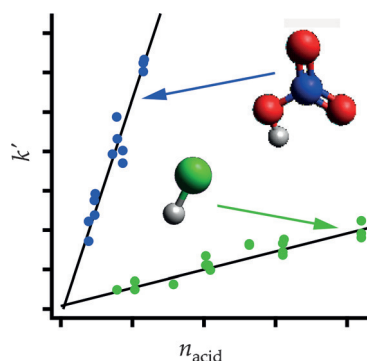
for sensitive functional groups. The preliminary mechanistic study suggests that a single electron transfer pathway is operative.

**Gas-Phase Reactions**

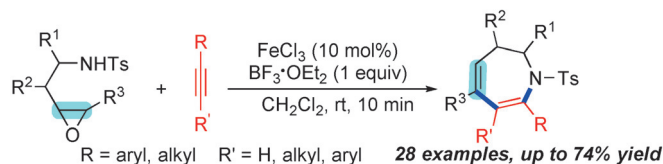
E. S. Foreman, K. M. Kapnas,
C. Murray* 10419–10422



Reactions between Criegee Intermediates and the Inorganic Acids HCl and HNO₃: Kinetics and Atmospheric Implications



Novel sink for Criegee intermediates: The rate constants for the reaction of the simplest Criegee intermediate, CH₂OO, with HCl (in green) and HNO₃ (in blue) were directly measured by broadband transient absorption spectroscopy. Both reactions occur at or near the collision limit, as was also confirmed by quantum-chemical calculations.



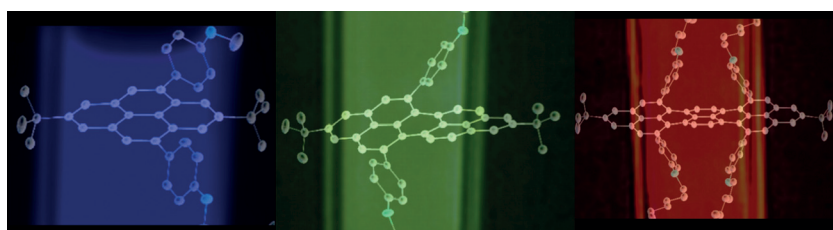
Access all azepines: An FeCl_3 and $\text{BF}_3 \cdot \text{OEt}_2$ co-catalyzed tandem hetero-[5+2] cycloaddition of 2-(2-aminoethyl)oxiranes with alkynes is presented. This method provides a rapid and practical

access to 2,3-dihydro-1*H*-azepines with exquisite chemo- and regiocontrol. The reaction is simple and has broad substrate scope and excellent functional-group tolerance.

Cycloaddition Reactions

C. Hu, R.-J. Song, M. Hu, Y. Yang, J.-H. Li,*
S. Luo* ————— **10423 – 10426**

[5+2] Cycloaddition of 2-(2-Aminoethyl)oxiranes with Alkynes via Epoxide Ring-Opening: A Facile Access to Azepines



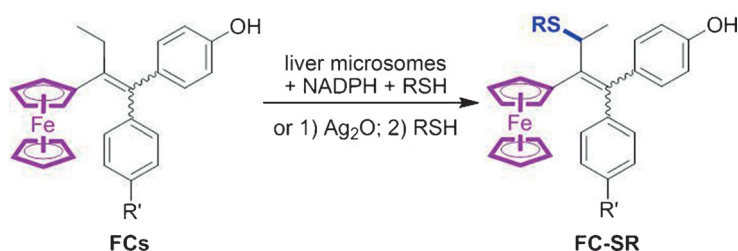
Pyrenes with a twist: The synthesis of soluble pyrenes, peropyrenes, and teropyrenes using a two- and fourfold alkyne benzannulation reaction promoted by Brønsted acid is reported. The compounds show an expected red shift in absorbance and emission as a function of

conjugation length with quantum yields of up to 62%. X-ray crystallographic analysis of these polycyclic aromatic hydrocarbons shows significant twisting of the aromatic core, thus demonstrating how flexible nanographenes can be.

Annulations

W. Yang, J. H. S. K. Monteiro,
A. de Bettencourt-Dias, V. J. Catalano,
W. A. Chalifoux* ————— **10427 – 10430**

Pyrenes, Peropyrenes, and Teropyrenes: Synthesis, Structures, and Photophysical Properties



Ferrociphenol quinone methide-thiol adducts are potent organometallic antiproliferative compounds that result from the addition of thiols to ferrocenyl quinone methides. These FC-SR adducts were identified upon metabolism of

ferrociphenols (FCs) by liver microsomes in the presence of NADPH and thiols. They display unique oxidative behaviors that may inspire development of new organometallic anticancer drugs.

Antiproliferative Agents

Y. Wang, M.-A. Richard, S. Top,*
P. M. Dansette, P. Pigeon, A. Vessières,
D. Mansuy,* G. Jaouen* ————— **10431 – 10434**

Ferrocenyl Quinone Methide-Thiol Adducts as New Antiproliferative Agents: Synthesis, Metabolic Formation from Ferrociphenols, and Oxidative Transformation



Inside Back Cover

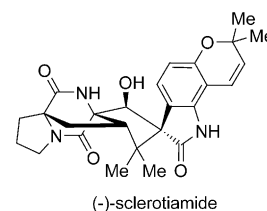
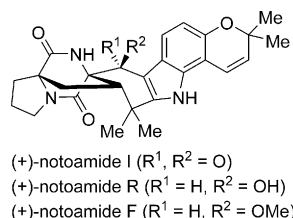


Indole Alkaloids

B. Zhang, W. Zheng, X. Wang, D. Sun,*
C. Li* 10435–10438



Total Synthesis of Notoamides F, I, and R and Sclerotiamide



Just a hop, skip, and a jump: The title compounds were synthesized in only 10–12 steps from the Seebach acetal. The synthetic approach features an oxidative aza-Prins cyclization to construct the

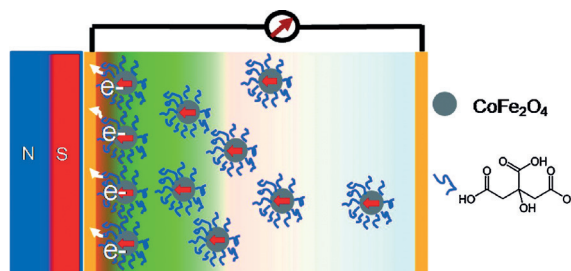
bicyclo[2.2.2]diazaoctane in a highly stereoselective manner and a cobalt-catalyzed radical cycloisomerization to build the cyclohexenyl ring.

Concentration Cells

Q. Dai, K. Patel, G. Donatelli,
S. Ren* 10439–10443



Magnetic Cobalt Ferrite Nanocrystals For an Energy Storage Concentration Cell



$CoFe_2O_4$ nanocrystals with controlled size and magnetic properties were synthesized. The energy storage performance of

concentration cells is dictated by the magnetic characteristics of the cobalt ferrite nanocrystal carriers.

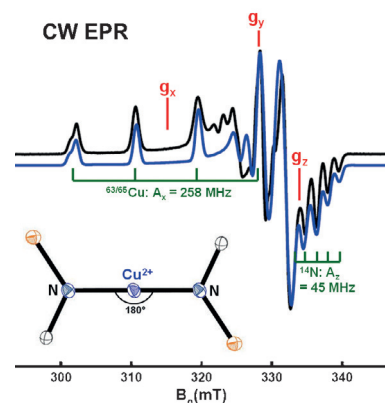
Copper Complexes

C. L. Wagner, L. Tao, E. J. Thompson,
T. A. Stich, J. Guo, J. C. Fetters,
L. A. Berben, R. D. Britt, S. Nagase,
P. P. Power* 10444–10447



Dispersion-Force-Assisted Disproportionation: A Stable Two-Coordinate Copper(II) Complex

Straight-up copper: The synthesis of the first linear Cu^{II} complex $Cu\{N(SiMe_3)Dipp\}_2$ ($Dipp = C_6H_5-2,6Pr_2$) and its Cu^I counterpart $[Cu\{N(SiMe_3)Dipp\}_2]^+$ is described. The former, studied by EPR spectroscopy, forms through a dispersion force-driven disproportionation, and is the reaction product of a Cu^I halide and $LiN(SiMe_3)Dipp$ in a non-donor solvent. The latter forms by preventing the disproportionation by using the complexing agent 15-crown-5.

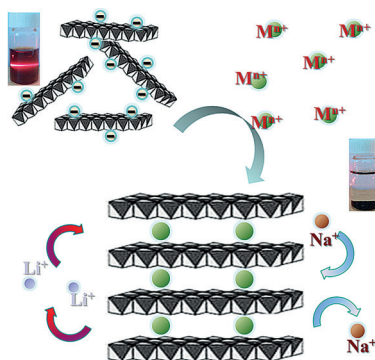


Electrochemistry

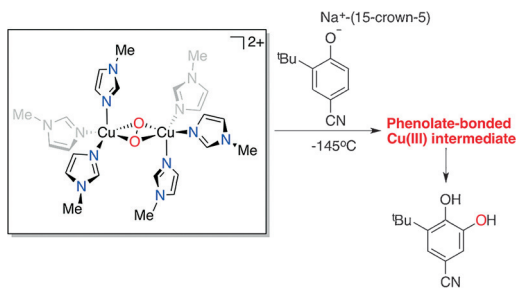
K. Lu, Z. Hu, Z. Xiang, J. Ma, B. Song,
J. Zhang,* H. Ma* 10448–10452



Cation Intercalation in Manganese Oxide Nanosheets: Effects on Lithium and Sodium Storage



Spoilt for choice: A series of three-dimensional M_xMnO_2 ($M = Li, Na, K, Mg$, or Co) cathodes with a sandwich structure were obtained by the self-assembly of manganese oxide nanosheets with these metal cations. The intercalated cations influence the capacity and cycling stability of these cathodes for lithium and sodium storage.



Cold copper cores: Three $N\pi$ -imidazole-bonded $\text{Cu}^{\text{II}}_2\text{O}_2$ species were synthesized and characterized at low solution temperatures. These complexes resemble the catalytic cores of tyrosinases, and allowed

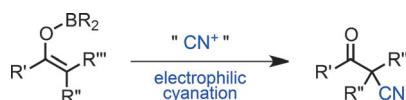
phenolate-ligated Cu^{III} intermediates during hydroxylation reactions to be probed, providing insights into the enzymatic mechanisms.

Coordination Chemistry

L. Chiang, W. Keown, C. Citek,
E. C. Wasinger,
T. D. P. Stack* ————— 10453 – 10457

Simplest Monodentate Imidazole
Stabilization of the oxy-Tyrosinase Cu_2O_2
Core: Phenolate Hydroxylation through
a Cu^{III} Intermediate

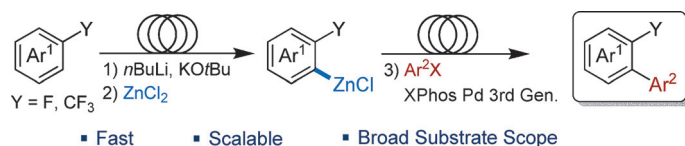
Plus CN: The title reaction proceeds with readily available cyanating reagents, *N*-cyano-*N*-phenyl-*p*-toluenesulfonamide and *p*-toluenesulfonyl cyanide. Various β -ketonitriles can be prepared by this new protocol, which shows a remarkably broad substrate scope compared to existing methods. The present method also allowed efficient synthesis of β -ketonitriles bearing a quaternary α -carbon center.



Synthetic Methods

K. Kiyokawa,* T. Nagata,
S. Minakata* ————— 10458 – 10462

Electrophilic Cyanation of Boron Enolates:
Efficient Access to Various β -Ketonitrile
Derivatives



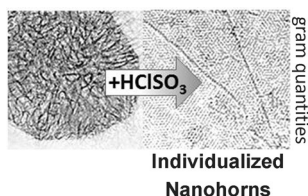
Hey! Ho! Let's flow! A highly regioselective functionalization of fluoro- and trifluoromethyl-substituted arenes and pyridines under continuous-flow conditions is described. This method telescopes

a directed lithiation, a zincation, and a Negishi cross-coupling into a single process to provide diversely functionalized, pharmaceutically relevant biaryls.

Flow Chemistry

S. Roesner,
S. L. Buchwald* ————— 10463 – 10467

Continuous-Flow Synthesis of Biaryls by
Negishi Cross-Coupling of Fluoro- and
Trifluoromethyl-Substituted
(Hetero)arenes



I am an individual: A facile approach for the separation of aggregated carbon nanohorns (CNHs), by treatment with chlorosulfonic acid, leads to p-doped species. The acid induces positive charges on the nanohorns which repel and push the individual nanohorns apart. The method yields gram quantities of free nanohorns.

Carbon Nanohorns

A. Stergiou, Z. Liu, B. Xu, T. Kaneko,
C. P. Ewels, K. Suenaga, M. Zhang,
M. Yudasaka,
N. Tagmatarchis* ————— 10468 – 10472

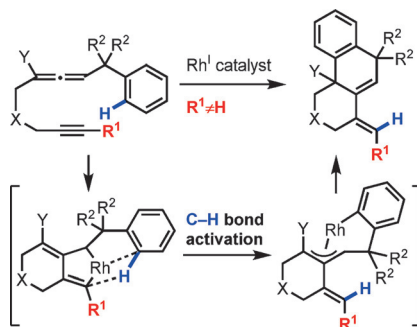
Individualized p-Doped Carbon
Nanohorns

Cycloisomerizations

Y. Kawaguchi, S. Yasuda,
C. Mukai* ————— 10473 – 10477



Construction of Hexahydrophenanthrenes
By Rhodium(I)-Catalyzed Cycloiso-
merization of Benzylallene-Substituted
Internal Alkynes through C–H Activation



Hexahydrophenanthrene derivatives were obtained from internal alkynes with a pendant benzylallene moiety through cycloisomerization by C(sp²)–H bond activation. The reaction likely proceeds by formation of a rhodabicyclo[4.3.0] intermediate, σ -bond metathesis between a C(sp²)–H bond on the benzene ring and the C(sp²)–Rh bond, and isomerization between three σ -, π -, and σ -allyl-rhodium(III) species.

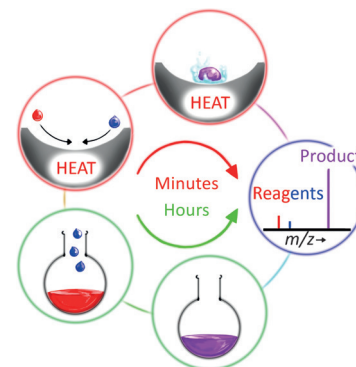
Reaction Kinetics

R. M. Bain, C. J. Pulliam, F. Thery,
R. G. Cooks* ————— 10478 – 10482



Accelerated Chemical Reactions and
Organic Synthesis in Leidenfrost Droplets

Chemical reactions can be accelerated in Leidenfrost levitated droplets in processes that are similar to reaction acceleration in charged microdroplets produced by electrospray ionization. Acceleration factors of 2 to 50 compared to the corresponding bulk-phase reactions were achieved for a range of transformations.

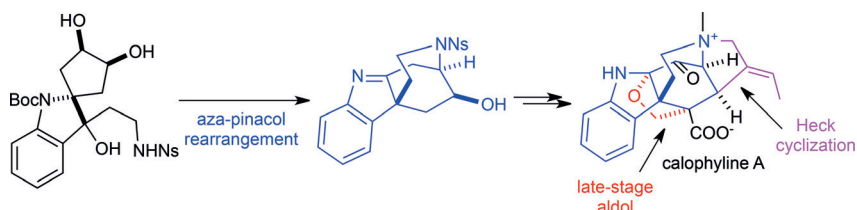


Natural Products

G. Li, X. Xie, L. Zu* ————— 10483 – 10486



Total Synthesis of Calophylline A



It has a nice ring: The first total synthesis of calophylline A is reported. The synthetic route features several key transformations, including an aza-pinacol rearrangement to construct the nitrogen-containing bridged [3.2.2] bicycle, a Heck cyclization

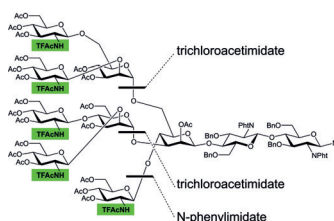
to assemble the fused 6/5/6/5 ring system, and a challenging late-stage aldol reaction to generate both a neopentyl quaternary stereogenic center and an oxygen-containing bridged [3.2.1] bicycle.

Glycans

M. Mönnich, S. Eller, T. Karagiannis,
L. Perkams, T. Luber, D. Ott, M. Niemietz,
J. Hoffman, J. Walcher, L. Berger,
M. Pischl, M. Weishaupt, C. Wirkner,
R. G. Lichtenstein,
C. Unverzagt* ————— 10487 – 10492

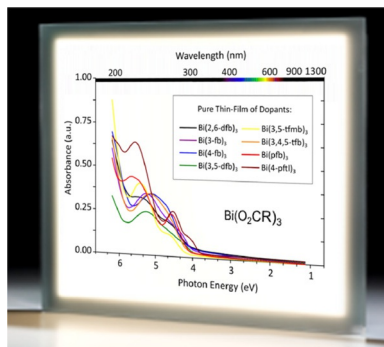


Highly Efficient Synthesis of
Multiantennary Bisected N-glycans
Based on Imidates



Bisecting á la carte: A general and robust modular approach to bisected N-glycans was established based on a unified protecting-group pattern. The switch to N-TFAc protection of the donors for the antennae provides high yields for the

difficult late-stage introduction of a bisecting GlcNAc. Regardless of the number of antennae, a judicious choice of imidate activation permits the highly efficient one-pot synthesis of bisected N-glycans.



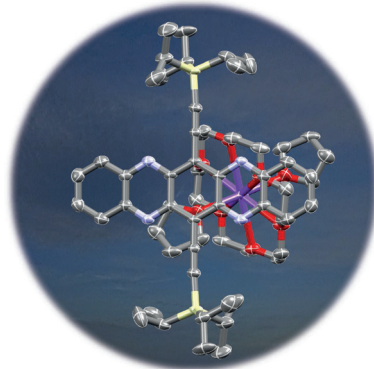
Bi doping: Ten new efficient p-dopants for conductivity doping of organic semiconductors for OLEDs are identified. The key advantage of the electrophilic tris(carboxylato)bismuth(III) compounds is the unique low absorption of the resulting doped layers. The combination of this feature with their low fabrication cost, volatility, and stability, make these materials very attractive as dopants in organic electronics.

Organic Semiconductors

S. Pecqueur, A. Maltenberger, M. A. Petrukhina, M. Halik, A. Jaeger, D. Pentlehner, G. Schmid* — 10493 – 10497

Wide Band-Gap Bismuth-based p-Dopants for Opto-Electronic Applications

Charged but not pinned down! The reduction of the symmetrical tetraazapentacene with potassium metal in THF gives the radical anion, a species critical in charge transport in field effect transistors. The negative charge is shown to be equally distributed over the whole molecule and not localized or pinned on the electro-negative nitrogen atoms.

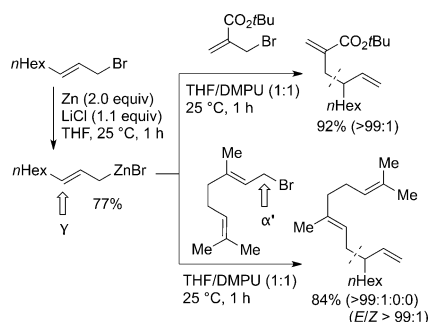


Azapentacene

L. Ji, M. Haehnel, I. Krummenacher, P. Biegger, F. L. Geyer, O. Tverskoy, M. Schaffroth, J. Han, A. Dreuw, T. B. Marder,* U. H. F. Bunz* — 10498 – 10501

The Radical Anion and Dianion of Tetraazapentacene

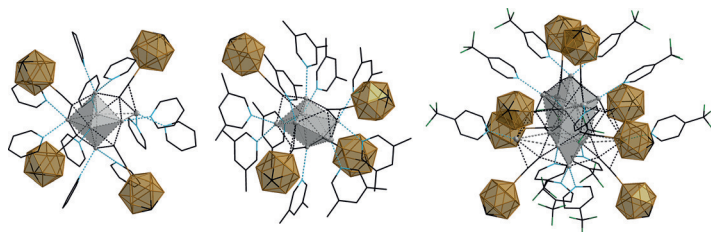
One of four possible products: Cross-coupling reactions of allylic zinc halides with allylic bromides provide 1,5-dienes with high regioselectivity. Various functional groups (ester, nitrile) are tolerated. Propargylic and benzylic halides can be used in this transformation. DFT calculations confirm the importance of LiCl for the efficient cross-coupling.



Synthetic Methods

M. Ellwart, I. S. Makarov, F. Achraier, H. Zipse, P. Knochel* — 10502 – 10506

Regioselective Transition-Metal-Free Allyl-Allyl Cross-Couplings



Six silver(I) clusters with five electronically different pyridine ligands were obtained starting from the silver(I) alkynyl $\{Ag_2(12-C\equiv C-closo-1-CB_{11}H_{11})\}_n$. All of the clusters show room-temperature phosphores-

cence, which is highly unusual for this class of compounds. A distorted pentagonal bipyramidal Ag_7^+ cluster with 3,5-lutidine gave a quantum yield of $\Phi = 0.76$, unprecedented for Ag^+ clusters.

Silver Clusters

M. Hailmann, N. Wolf, R. Renner, T. C. Schäfer, B. Hupp, A. Steffen,* M. Finze* — 10507 – 10511

Unprecedented Efficient Structure Controlled Phosphorescence of Silver(I) Clusters Stabilized by Carba-closo-dodecaboranylethynyl Ligands

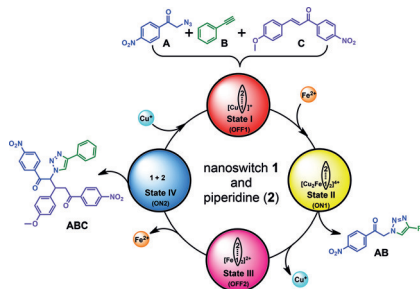


Sequential Catalysis

S. Gaikwad, A. Goswami, S. De,
M. Schmittle* _____ 10512–10517



A Metalloregulated Four-State
Nanoswitch Controls Two-Step Sequential
Catalysis in an Eleven-Component System



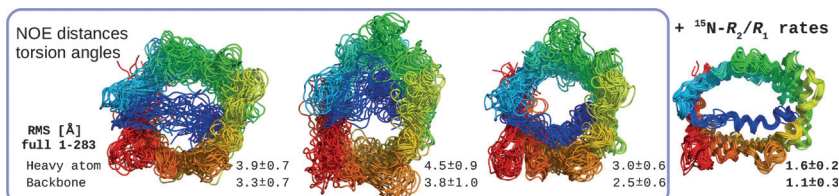
Connect four: The first nanoswitch with four states can control a sequential transformation $A + B + C \rightarrow AB + C \rightarrow ABC$ with 11 components over two complete cycles. The cycle proceeds stepwise along the switching states OFF1 \rightarrow ON1 (click reaction: $A + B \rightarrow AB$) \rightarrow OFF2 \rightarrow ON2 (Michael addition: $AB + C \rightarrow ABC$) \rightarrow OFF1 (see scheme). The system's performance is superior to that of systems with only two switching states.

NMR Spectroscopy

M. Jaremko, Ł. Jaremko, S. Villinger,
C. D. Schmidt, C. Griesinger, S. Becker,
M. Zweckstetter* _____ 10518–10521



High-Resolution NMR Determination of
the Dynamic Structure of Membrane
Proteins



Just relax: ^{15}N nuclear magnetic relaxation was used to determine the 3D structure of a challenging membrane protein. The structure of the human voltage-dependent anion channel refined to high resolution

against relaxation rates shows unique features of an anisotropically shaped barrel and a well-folded N-terminal helix.



Supporting information is available
on www.angewandte.org
(see article for access details).



A video clip is available as Supporting
Information on www.angewandte.org
(see article for access details).



This article is available online free of
charge (Open Access).



This article is accompanied by a cover
picture (front or back cover, and inside
or outside).

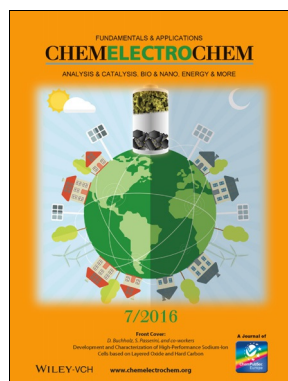


The Very Important Papers, marked
VIP, have been rated unanimously as
very important by the referees.

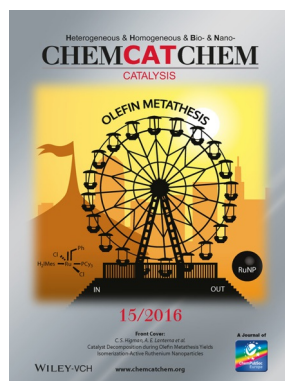


The Hot Papers are articles that the Editors
have chosen on the basis of the referee
reports to be of particular importance for
an intensely studied area of research.

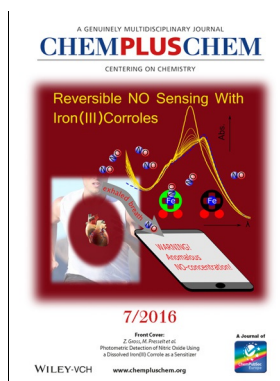
Check out these journals:



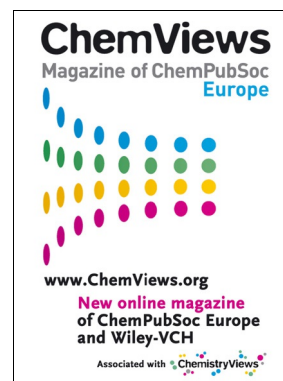
www.chemelectrochem.org



www.chemcatchem.org



www.chempluschem.org



www.chemviews.org